

SIMULATIONS OF MECHANICAL PROPERTIES FOR DISCONTINUOUS PREPREG COMPOSITES - 075

*Denos, Benjamin R., Kravchenko, Sergii G., Pipes, R. Byron
Composites Manufacturing & Simulation Center, Purdue University, West Lafayette, IN*

Abstract

Discontinuous prepreg composites, sometimes known as chopped, randomly oriented strand, or prepreg platelet molding compound (PPMC), are challenging to model due to their heterogeneity at multiple scales. While highly ordered morphologies can be obtained with these material systems, more often an uncontrolled orientation state in the platelets creates high variability in the local and macro mechanical response. The reinforcing fiber orientation is integral to predicting performance as it is with continuous fiber composites. However, for PPMCs it is important to know orientation at the mesoscale, or platelet-scale, instead of just a few ply angles because that mesoscale morphology is locally variable in plane and through the thickness. The presented research uses orientation measurements from x-ray tomography to inform FE models for progressive failure analysis. Both direct-orientation-mapped virtual twins of CT scanned specimens and virtually generated specimen FE models with measurement-informed orientation states are used to successfully predict elastic and failure responses of Dow M6400 molded PPMC tensile bars from flat plaques and flat portions of other molded geometries. The virtual twins allow for validation of the modeling method against experimental results, and the virtually generated specimens allow for exploration of the material system design space such as geometry thickness and platelet size.

Background

In order to fill the niche between injection molded fiber reinforce composites and continuous fiber laminates, a number of different sheet molding compounds (SMCs) and bulk molding compounds (BMCs) have been developed over the previous decades [1]. A newer form of SMC, here called prepreg platelet molding compound (PPMC), has been developed to fill out the upper performance range of SMCs by creating the platelets from cut and slit unidirectional prepreg tape. This work is specifically focused on the Dow Vorafuse™ M6400 material system. The platelets inherit the initial fiber alignment and fiber volume fraction from their parent tape, but the system has sufficient discontinuity to be employed in a molding process. Both thermoplastic and thermoset matrices can be used, but rapid cure thermosets show more promise for the fast cycle time requirements of the automotive industry. The discontinuity and orientation state of platelets can be controlled, but platelets are typically deposited into a charge that is uncontrolled, leading to a large degree of morphological and performance variability [2]–[4]. There are some unique characteristics of PPMCs that demand different design and simulation considerations than engineers may be used to with other composite material systems.

Unique Mesostructure and Morphology of PPMCs

Platelets cut from unidirectional prepreg tape have a thickness to match the prepreg, but length and width can be designed as desired. Typically, length > width > thickness to promote efficient stress transfer from platelet to platelet, where the intra-platelet unidirectional fibers are along the length direction as shown in Figure 1a. While platelets deform through shearing and bending mechanisms, all micrograph based observations of this work showed that they remain intact as locally aligned fiber bundles. Relatively few fibers completely disaggregate from their platelet/fiber bundle to assume a separate and unique orientation state. This has been observed

for low and medium flow length scenarios [5]. Therefore, the final molded morphology of a PPMC-based composite geometry consists of high fiber volume fraction aligned fibers at the microscale within each platelet, intra-platelet continuous smooth orientation state, inter-platelet orientation discontinuity, and a highly variable distribution of orientations from the platelet mesoscale up to the specimen macroscale. For planar geometries, this orientation state variability is present both in plane and through the thickness as seen in the inspection region of a flat plaque in Figure 1b.

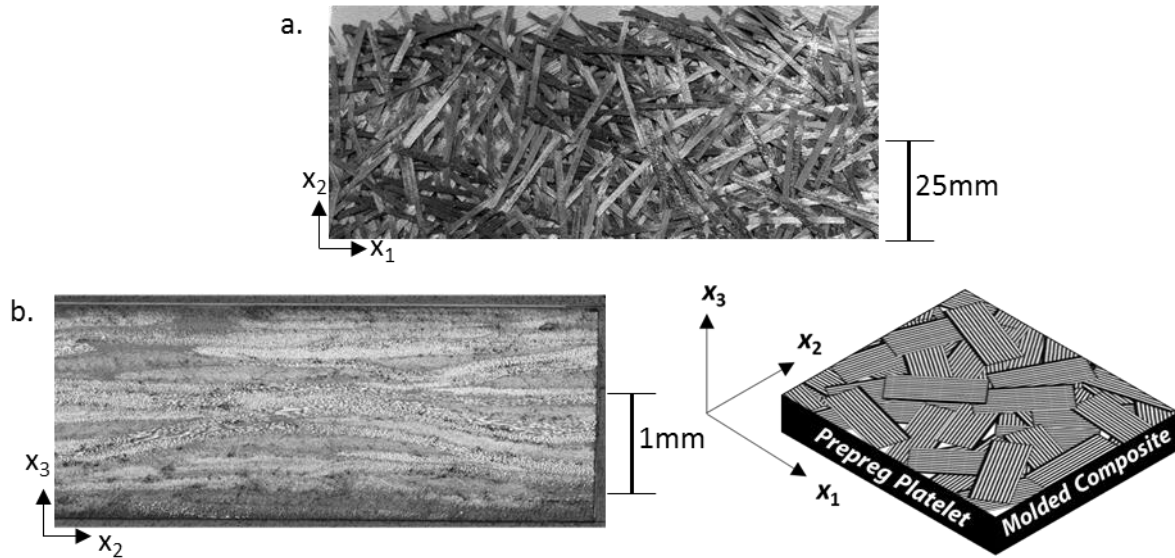


Figure 1. a) Unconsolidated Prepreg Platelet Molding Compound Mat, b) Micrograph and Diagram of Consolidated PPMC Plaque

If one is to simulate the mechanical response of such a complex material system it seems desirable to make assumptions in order to simplify the task. Microscopy inspection work by this research group and others [6]–[11] exhibit morphological features that should clearly affect elastic and strength performance, including platelet deformation and thickness changes. As with all fiber reinforced composites the fiber orientation has a large influence on local and macro stiffness and strength. The platelet thickness also plays a critical role in the ability of any stacked and staggered platelet morphology to effectively transfer stress through and around the mesostructure. Platelet orientation and thickness may be measured via microscopy to determine statistical variability, but planar micrographs do not tell the complete story of any given specimen due to the extreme local morphology variability. In order to characterize morphology over a larger, specimen-scale domain computed tomography scans of entire specimens are analyzed.

CT-Based Orientation Analysis

X-ray CT scanning is featured in an increasing number of composite studies as the technology becomes more available. Just as important as the CT scan technology itself is development of methodologies to interpret the relative density data for specific composite applications. CT scans have been used to characterize failure mechanisms [12], [13], defects [14]–[16], short fiber material systems [17], [18], woven composites [7], [19], fiber waviness [20], and various forms of SMCs including PPBCs [21]. Some of these studies study limited volumes of a few mm^3 in order to see individual fibers, others scan larger plaques or geometries, but sacrifice resolution to image these volumes. The unique morphology of PPBCs studied here allow for determination of mesoscale details from CT scan resolutions on the order of a half platelet thickness ($50\mu\text{m}$) or less, which can be obtained for volumes like that of a tensile coupon ($152 \times 25 \times 3\text{mm}$).

For more complete details on the use of mesoscale CT scans to determine platelet orientation in PPMC see [22]. The cited works discuss both a Matlab-based orientation analysis and one using the commercial software from Volume Graphics [23]. This work will use results from Volume Graphics VGStudio MAX software. In simplified terms, the CT scan must be captured with sufficient resolution and contrast to discern the intra- and inter-platelet density gradients which can be used to identify the direction of smallest density gradient as the fiber direction and the direction of greatest density gradient as the platelet normal direction. Although platelets may deform, the fact that they remain as bundles of similarly oriented fibers allows this correlation of density gradient to platelet orientation, which includes the constituent fiber orientation. There are some challenges to consider with the very large density gradients near boundaries, voids, and resin rich regions, but in comparison with capturing the fiber orientation state these other qualities have had minimal impact on modeling.

Previous Simulation Approaches for PPMCs

There are a number of studies that use various measurements and models to simulate the behavior of PPMC-like material systems. Feraboli et al. use a stochastic laminate analogy with random representative volume elements (RRVE) to generate a virtual specimen of regularly spaced shell elements that embody a PPMC's variable properties by assigning random laminate definitions to each element [3] Harper et al. addressed the issue of determining effective RVE size for long discontinuous fibers that highlight the importance of retaining critical mesoscale features that approach the macroscale of a specimen by selective homogenization [24]. Harban and Tuttle implement a representative laminate volume element (RLVE) model to explore stiffness, strength, and notched strength with success for estimating mean values for elastic and failure response, although stiffness variability does not seem as extreme in the predictions as in their experimental data [25]. Their low (computational) cost approach shows the value of simulation for design and certification that this work hopes to continue with a morphology model of greater complexity and the use of solid FE elements.

Like all simulations, these examples rely on assumptions to make the solution more tractable. The presented work utilizes the assumption that a single orthotropic material model applied to the orientation-informed elements of an FE model captures the morphology critical to simulation of PPMCs. The effect of platelet thickness is inherent in CT based models, and can be tested in virtually generated specimens. Three separate approaches are being actively researched at the Composites Manufacturing and Simulation Center (CMSC) at Purdue University to match simulated performance with experimental performance, but only two are discussed in this paper: CT-based virtual twins and virtually generated test specimen models. Figure 2 shows the three workflow options being developed.

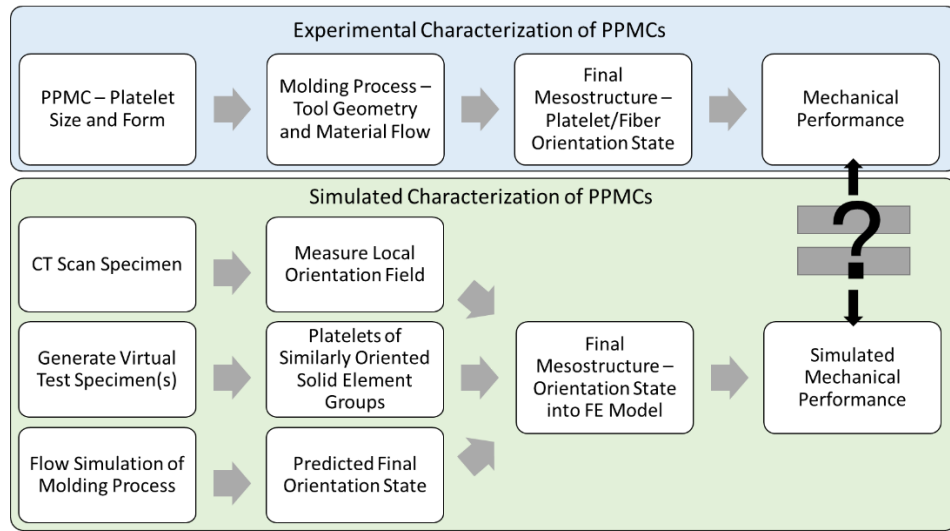


Figure 2. Workflow Options for Simulation of PPMCs

CT-Based Virtual Twin FE Models

CT scans of tensile specimens have been performed by Delphi Precision Imaging in Redmond Washington and by The University of Tennessee Knoxville and Volume Graphics VG Studio MAX was used to perform an integration mesh orientation analysis of the scan volumes. As stated previously, scans must be performed such that the density gradients are discernible at the sub-platelet scale but are unlikely to reach a scale that can resolve fibers when scanning a coupon-sized geometry. This full-geometry data is powerful because it contains all the morphological information available at the mesoscale, including platelets with their flow-induced shape and thickness deformations. An example of one slice from a CT scan with sufficient resolution and contrast is shown in Figure 3.

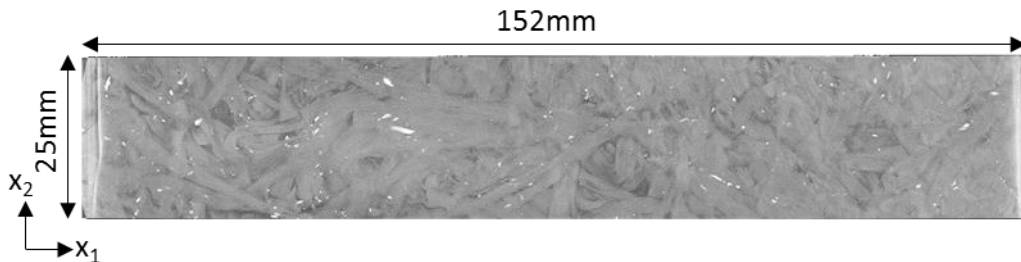


Figure 3. CT Scan Slice of Tensile Specimen Gage Region, 39 μ m Resolution

In VGStudio an integration mesh of hexahedral elements of size 0.7x0.7x0.1mm is created to envelope the volume of interest. Gradient based analysis is performed in each integration mesh element and an orientation tensor is calculated, along with the principal vectors of that tensor via Eigen analysis. A Matlab code is used to generate an Abaqus input file from the VGStudio output to apply the principal vectors as the material coordinate system for each element. The additional information present in the orientation tensor data could be used to more specifically tailor the material properties of each element, but for this work only the principal vectors are applied as the orthotropic fiber, transverse, and platelet normal directions. This results in an FE model with a single orthotropic material definition, but each element has a unique, measurement-based material coordinate system as seen with the vectors in Figure 4.

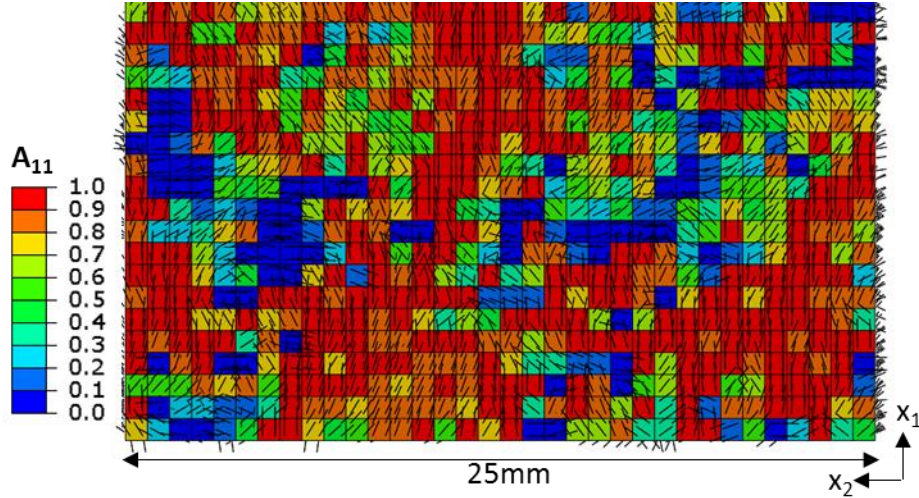


Figure 4. CT-Based FE Model Section with A_{11} (~Axial Alignment) and Element Material Fiber Orientation Vectors

What has been created is a CT-informed virtual twin that contains the local mean orientations of the scanned specimen as well as the variable thickness of platelets if a sufficiently fine through thickness mesh size is chosen. Element size is chosen such that each one can contain a single orientation state with reasonable accuracy. Because the CT scan analysis is nondestructive, there is opportunity for a 1:1 comparison with experiment. This is helpful to establish modeling practices for PPMCs. Specifically, one can determine the effective orthotropic material properties that should be applied to each element. The element size in virtual twins here allows the use of the parent tape material properties given in Table 1 since the discontinuities between platelets are captured as transitions by the spatial transitions of orientation state. A 3D stress, 3D damage Hashin Tsai progressive damage criterion is applied to the material model, allowing for progressive failure of the continuum model elements when critical stresses or strains are reached. For more modeling details see similar work in [26].

Table 1. Material Properties Used in Simulations

Property	Value	Property	Value
X_1 (MPa)	1654 ± 17.8	E_1 (GPa)	141.7 ± 1.54
X_2 (MPa)	58.6 ± 2.7	E_2 (GPa)	7.44 ± 0.25
S_6 (MPa)	91.7 ± 5.6	G_{12} (GPa)	5.73 ± 0.53
0/ $\pm 45/90$ Strength (MPa)	487.0 ± 48.7	0/ $\pm 45/90$ Modulus (GPa)	40.2 ± 3.18
Mode I Fracture Toughness (J/m ²)	606 ± 32.41	v_{12}	0.32 ± 0.01

Boundary conditions for each virtual twin are set up as a tensile test with one end of the specimen fixed and one subjected to a displacement equivalent to a 1.2% strain. Simulation results show a damage location that compares favorably with the experimental results as seen in Figure 5.

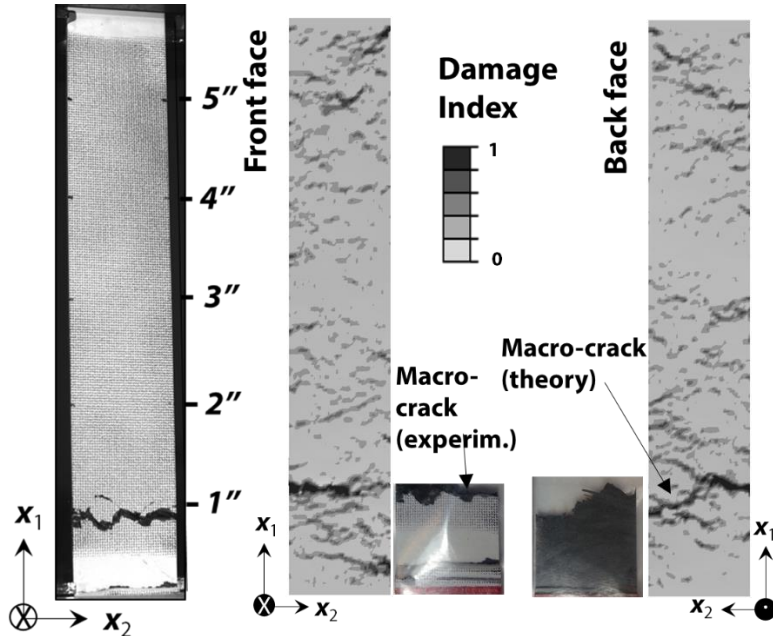


Figure 5.1: Comparison of Experimental and CT Virtual Twin Damage from Tensile Test

It is important to note that the strain response of one face of the experimental bar, as simulated or measured by digital image correlation (DIC), may vary considerably from the strain response of the opposite face. As stated previously, the orientation state can vary both in plane and through thickness, which will manifest as different mean and local strains on each surface. Simulation contains the full strain response through the thickness so it is best to collect experimental strain response data on both surfaces when possible. Initially, this test series did not appear to have a strong stress-strain match between the simulations and experimental results, which were performed with DIC only on the “front” face of the specimen. Examination of the changing orientation state through the thickness of the virtual twin led to an alternative analysis of the simulation data where strain response was measured from each surface, as if performed by virtual DIC. A plot containing both surface based mean strains, the full bar simulation response, and the experimental response from the front face is shown in Figure 6 to demonstrate the variation in strain (and calculated modulus) depending on which side of the specimen is used.

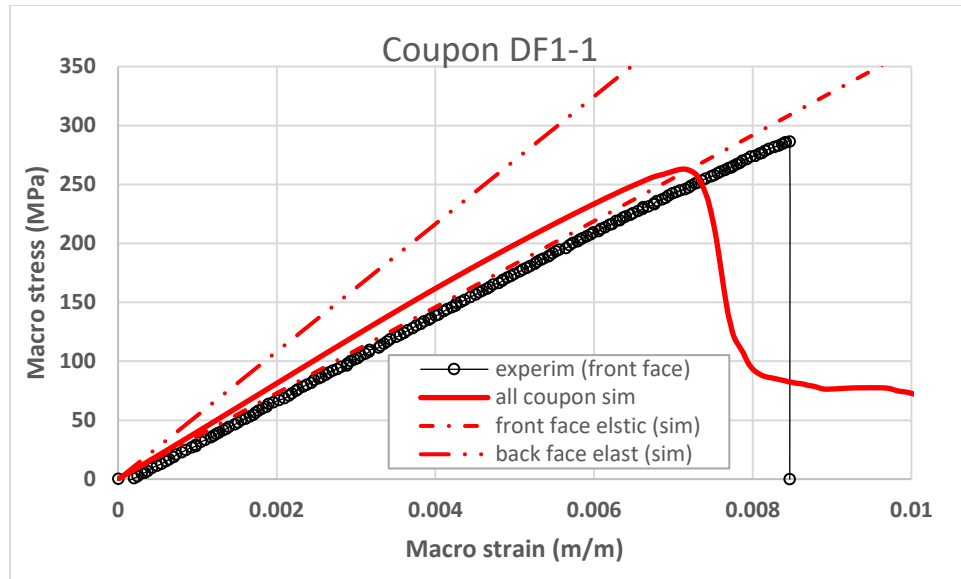


Figure 6. DIC-Calculated Experimental Response at Front Face VS. Virtual Twin Response at Front/Back Faces and for Entire Specimen

When making the more direct comparison of surface strain from the simulation and from DIC of the same face, the results began to correspond more clearly. Of special note is the large difference in strain response along the virtual “back” face of the specimen, which has significantly greater stiffness (54GPa) than the “front” face (36GPa). While this test series was performed experimentally with DIC only on one face, later tests of PPMC specimens with similar thicknesses showed front to back DIC-measured variations in calculated tensile modulus of 20GPa are not unreasonable. Not every specimen will have such a large variation, but the possibility should be acknowledged and accounted for by choosing carefully the strain measurements that will be compared between simulation and experimental results. Preferably, DIC data will be taken from both surfaces for all future tests so that a more complete set of experimental data can be compared with simulation predictions.

Virtually Generated FE Models with Discrete Platelets

While CT-based virtual twins allow for direct 1:1 comparisons with single experimental specimens and study of regional morphology variability, they are relatively costly. It is preferable to create a completely virtual series of specimens if they can be made to contain the important morphological features realistic to PMPCs. In fact, virtually building an FE model allows for creation of uniquely oriented platelets and the inclusion of explicit platelet boundaries as seen in Figure 7. More modeling details for similar work can be found in [27].

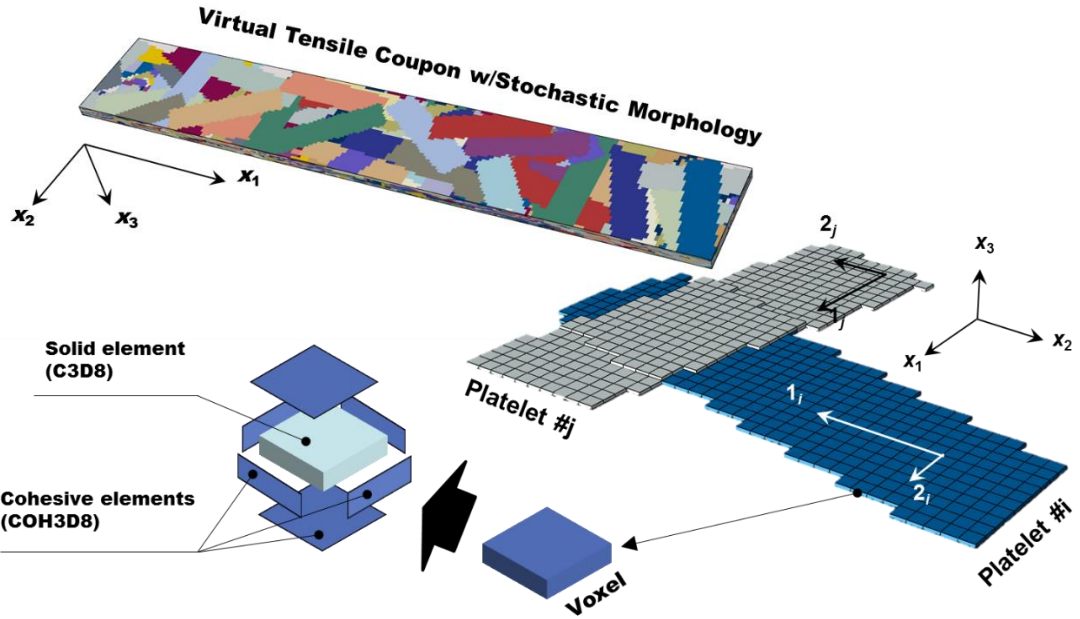


Figure 7. Virtually Generated Tensile Specimen with Platelet Element Groupings and Cohesive Elements

As illustrated, using a tool like e-Xstream Digimat FE, an entire virtual coupon can be created with platelets represented by groupings of elements with similar local material orientation and cohesive elements between platelets that allow for proper modeling of delamination failure mechanisms. The platelets generated are limited to a single thickness definition and rectangular shape that do not account for some of the platelet deformations observed via microscopy. The waviness of overlapping platelets is accounted for in step increments of one platelet thickness. The orientation selection for each platelet in Digimat is governed by the user input of orientation tensor A_{ij} , which is used to create an approximate distribution function via standard closure techniques [28].

Microscopy measurements in Figure 8 illustrate a variability of platelet thicknesses present in a plaque geometry such that choosing a single thickness definition for any model may misrepresent the range of performance that will be observed in reality. A study was performed where platelet thickness was assumed to be 0.08mm for one set of five specimens and 0.1mm for a second set. The results in Figure 8 illustrate the ability of thinner platelets increase the average specimen strength.

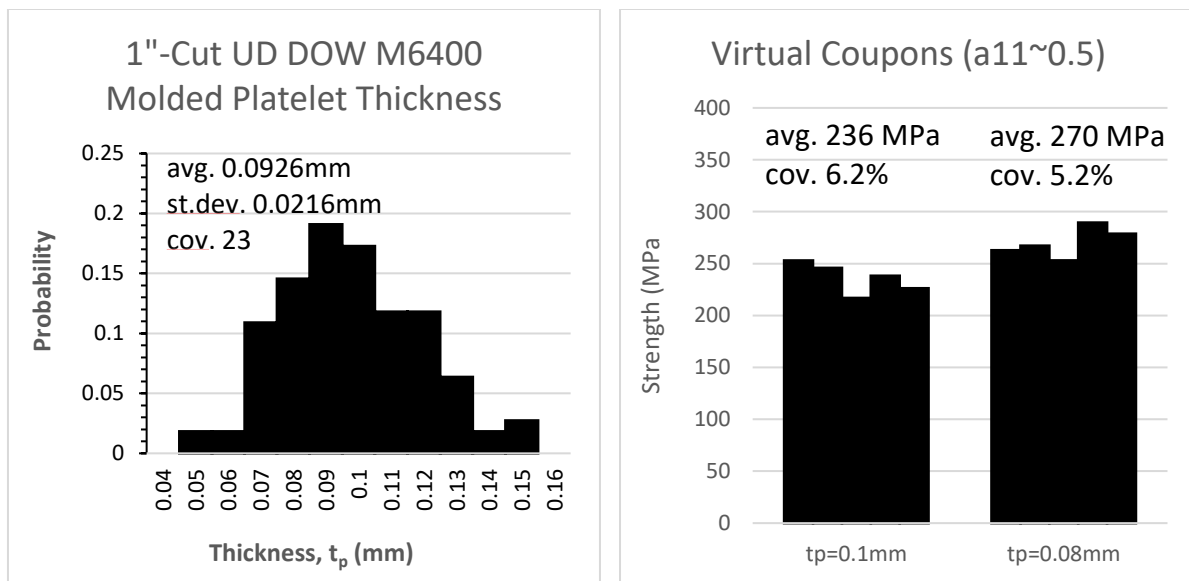


Figure 8. Molded Platelet Thickness Distribution and Effect of Platelet Thickness on Strength

It is suggested to similarly determine variability in platelet thickness for any new manufacturing parameters and to determine performance bounds with virtual sets by selecting two or more thicknesses for specimen generation. Single specimens cannot currently be generated with multiple platelet thicknesses using Digimat FE, although one can imagine ways to accomplish this improved model fidelity at the cost of finer mesh density. Even with the platelet shape, thickness, and orientation generation assumptions a series of these virtual coupons can be utilized to great benefit in designing and predicting performance of PPMCs. Using the same properties as the virtual twin specimens, the elastic and failure response of virtually generated bars, D_V-#, match a selection of the experimental results, M##-#, provided by Dow in Figure 9.

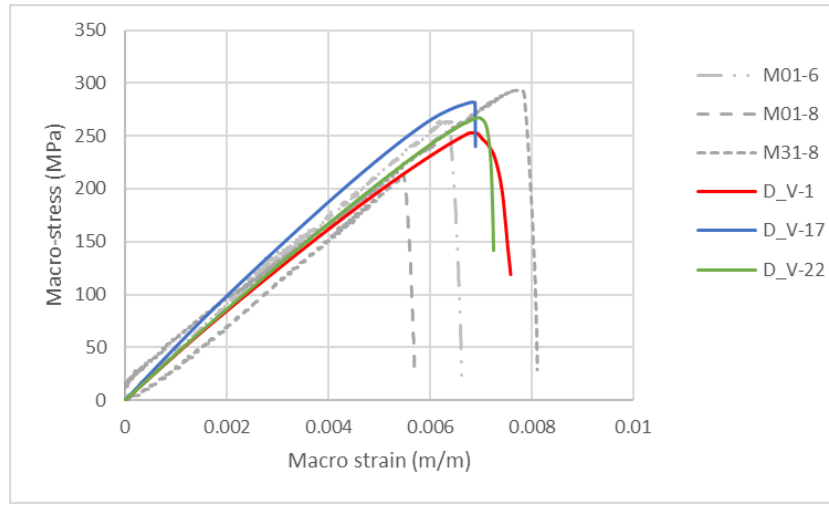


Figure 9. Select Virtual Tensile Specimen Responses (D_V) VS. Select Experimental Responses (M##-#)

The tensile modulus and strength are both captured well for the virtual specimens shown. When viewed as a bar chart in Figure 10 of simulated and experimental strengths for the full set of test data presently available the distribution of strengths shows comparable variability.

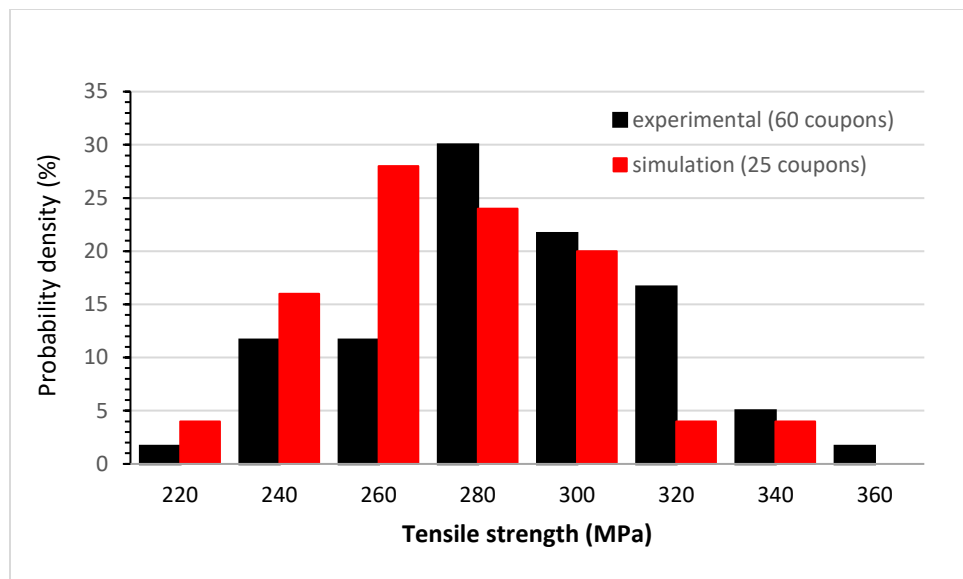


Figure 10. Strength Distribution of Virtual Specimen Tensile Test Series VS. Experimental

While the range of values shown may appear discouraging to designers at first, the ability to predict this range prior to physical testing allows designers to determine the effect of platelet geometry and orientation state in a new and powerful way for PPMCs.

Summary and Next Steps

Two methods for simulation of PPMC mechanical performance have been presented that consider the critical characteristics of platelet orientation state and thickness. For 1:1 experimental comparison, a CT-scan-based virtual twin model can be generated from measurements of local mean orientation state mapped onto an FE mesh. For a more statistical approach, a completely virtual test series of specimens can be generated, allowing greater exploration of the PPMC design space. Both models assign the same orthotropic material properties to each element according to the element's local material coordinate system. Next steps for the CT virtual twin method includes a convergence study for mesh density effects on local and macro response. For the virtual specimen method, the primary goal is to perform more analyses to explore the PPMC design space and compare with experimental data sets.

Acknowledgements

This work was sponsored by the Institute for Advanced Composites Manufacturing Innovation under Project 3.2.

Bibliography

- [1] V. P. McConnell, "New recipes for SMC innovation," *Reinforced Plastics*, vol. 52, no. 8, pp. 34–39, 2008.
- [2] P. Feraboli, E. Peitso, T. Cleveland, and P. B. Stickler, "Modulus Measurement for Prepreg-based Discontinuous Carbon Fiber/Epoxy Systems," *J. Compos. Mater.*, vol. 43, no. 19, pp. 1947–1965, 2009.
- [3] P. Feraboli, T. Cleveland, P. B. Stickler, and J. C. Halpin, "Stochastic laminate analogy for simulating the variability in modulus of discontinuous composite materials," *Compos. Part A Appl. Sci. Manuf.*, vol. 41, no. 4, pp. 557–570, 2010.
- [4] S. B. Visweswaraiyah, M. Selezneva, L. Lessard, and P. Hubert, "Mechanical characterisation and

- modelling of randomly oriented strand architecture and their hybrids – A general review,” *J. Reinforced Plast. Compos.*, vol. 37, no. 8, pp. 548–580, 2018.
- [5] B. R. Denos, “Fiber Orientation Measurements in Platelet-Based Composites via Computed Tomography Analysis,” Purdue University, 2017.
 - [6] R. S. Bay and C. L. Tucker, “Stereological Measurement and Error Estimates for Three-Dimensional Fiber Orientation,” *Polym. Eng. Sci.*, vol. 32, no. 4, pp. 240–253, 1992.
 - [7] F. Desplentere, S. V. Lomov, D. L. Woerdeman, I. Verpoest, M. Wevers, and A. Bogdanovich, “Micro-CT characterization of variability in 3D textile architecture,” *Compos. Sci. Technol.*, vol. 65, no. 13, pp. 1920–1930, 2005.
 - [8] R. Luchoo, L. T. Harper, M. D. Bond, N. A. Warrior, and A. Dodworth, “Net shape spray deposition for compression moulding of discontinuous fibre composites for high performance applications,” *Plast. Rubber Compos.*, vol. 39, no. 3–4, pp. 216–231, 2010.
 - [9] H. Salek and J. Denault, “Viscous Behavior of Resin and Flow Through the Fiber Network of Carbon / Pekk,” in *The 9th International Conference on Flow Processes in Composite Materials*, 2008, vol. 9, no. July.
 - [10] B. Landry and P. Hubert, “Experimental study of defect formation during processing of randomly-oriented strand carbon/PEEK composites,” *Compos. Part A Appl. Sci. Manuf.*, vol. 77, pp. 301–309, Oct. 2015.
 - [11] P. Feraboli, T. Cleveland, M. Ciccu, P. B. Stickler, and L. DeOto, “Defect and damage analysis of advanced discontinuous carbon/epoxy composite materials,” *Compos. Part A Appl. Sci. Manuf.*, vol. 41, no. 7, pp. 888–901, 2010.
 - [12] P. J. Schilling, B. R. Karedla, A. K. Tatiparthi, M. A. Verges, and P. D. Herrington, “X-ray computed microtomography of internal damage in fiber reinforced polymer matrix composites,” *Compos. Sci. Technol.*, vol. 65, no. 14, pp. 2071–2078, 2005.
 - [13] K. T. Tan, N. Watanabe, and Y. Iwahori, “X-ray radiography and micro-computed tomography examination of damage characteristics in stitched composites subjected to impact loading,” *Compos. Part B Eng.*, vol. 42, no. 4, pp. 874–884, 2011.
 - [14] A. Abdul-Aziz, C. Saury, V. Bui Xuan, and P. G. Young, “On the material characterization of a composite using micro CT image based finite element modeling,” *Nondestruct. Evaluation Heal. Monit. Diagnostics*, vol. 6176, no. APRIL, pp. 617605-617605–8, 2006.
 - [15] R. Stoessel, D. Kiefel, R. Oster, B. Diewel, and L. Llopard Prieto, “ μ -Computed Tomography for 3D Porosity Evaluation in Carbon Fibre Reinforced Plastics (CFRP),” *Int. Symp. Digit. Radiol. Comput. Tomogr.*, 2011.
 - [16] E. Weber, M. Fernandez, P. Wapner, and W. Hoffman, “Comparison of X-ray micro-tomography measurements of densities and porosity principally to values measured by mercury porosimetry for carbon-carbon composites,” *Carbon N. Y.*, vol. 48, no. 8, pp. 2151–2158, 2010.
 - [17] H. Shen, S. Nutt, and D. Hull, “Direct observation and measurement of fiber architecture in short fiber-polymer composite foam through micro-CT imaging,” *Compos. Sci. Technol.*, vol. 64, no. 13–14, pp. 2113–2120, 2004.
 - [18] M. W. Czabaj, M. L. Riccio, and W. W. Whitacre, “Numerical reconstruction of graphite/epoxy composite microstructure based on sub-micron resolution X-ray computed tomography,” *Compos. Sci. Technol.*, vol. 105, pp. 174–182, 2014.
 - [19] T. Centea and P. Hubert, “Measuring the impregnation of an out-of-autoclave prepreg by micro-CT,” *Compos. Sci. Technol.*, vol. 71, no. 5, pp. 593–599, 2011.
 - [20] S. Fliegener, M. Luke, and P. Gumbsch, “3D microstructure modeling of long fiber reinforced thermoplastics,” *Compos. Sci. Technol.*, vol. 104, pp. 136–145, 2014.
 - [21] Y. Wan, I. Straumit, J. Takahashi, and S. V Lomov, “Micro-CT analysis of internal geometry of

chopped carbon fiber tapes reinforced thermoplastics," *Compos. Part A*, no. 91, pp. 211–221, 2016.

- [22] B. R. Denos and R. B. Pipes, "Local mean fiber orientation via computer assisted tomography analysis for long discontinuous fiber composites," in *Proceedings of the American Society for Composites - 31st Technical Conference, ASC 2016*, 2016.
- [23] Volume Graphics GmbH, "VGSTudio MAX Brochure," 2017. [Online]. Available: https://www.volumegraphics.com/_Resources/Persistent/6247cd363d6a9c0336d52344d580d3630a07d0d9/VGSTUDIO_MAX_30_en.pdf. [Accessed: 17-Jun-2017].
- [24] L. T. Harper, C. Qian, T. A. Turner, S. Li, and N. A. Warrior, "Representative volume elements for discontinuous carbon fibre composites - Part 1: Boundary conditions," *Compos. Sci. Technol.*, vol. 72, no. 2, pp. 225–234, 2012.
- [25] K. Harban, M. Tuttle, and C. Davies, "CERTIFICATION OF DISCONTINUOUS FIBER COMPOSITES VIA STOCHASTIC MODELING," 2017.
- [26] B. R. Denos, S. G. Kravchenko, and R. B. Pipes, "Progressive failure analysis in platelet based composites using ct-measured local microstructure," in *International SAMPE Technical Conference*, 2017.
- [27] S. Kravchenko and B. Pipes, "Virtual tensile testing of prepreg platelet composite molded with stochastic morphology," in *SAMPE 2018*, 2018.
- [28] S. G. Advani and C. L. Tucker, "The Use of Tensors to Describe and Predict Fiber Orientation in Short Fiber Composites," *J. Rheol. (N. Y. N. Y.)*, vol. 31, no. 8, p. 751, 1987.